ALMA MATER STUDIORUM
UNIVERSITÀ DI BOLOGNA

ARCHIVIO ISTITUZIONALE
DELLA RICERCA

Alma Mater Studiorum Università di Bologna
Archivio istituzionale della ricerca

The mitochondrial F1FO-ATPase exploits the dithiol redox state to modulate the permeability transition pore

This is the final peer-reviewed author's accepted manuscript (postprint) of the following publication:

Published Version:
The mitochondrial F1FO-ATPase exploits the dithiol redox state to modulate the permeability transition pore / Algieri, Cristina; Trombetti, Fabiana; Pagliarani, Alessandra; Ventrella, Vittoria; Nesci, Salvatore. - In: ARCHIVES OF BIOCHEMISTRY AND BIOPHYSICS. - ISSN 0003-9861. - STAMPA. - 712:(2021), pp. 109027.1-109027.5. [10.1016/j.abb.2021.109027]

Availability:
This version is available at: https://hdl.handle.net/11585/832412 since: 2021-11-03

Published:

DOI: http://doi.org/10.1016/j.abb.2021.109027

Terms of use:

Some rights reserved. The terms and conditions for the reuse of this version of the manuscript are specified in the publishing policy. For all terms of use and more information see the publisher's website.

This item was downloaded from IRIS Università di Bologna (https://cris.unibo.it/).
When citing, please refer to the published version.

(Article begins on next page)

18 April 2024

This is the final peer-reviewed accepted manuscript of:

The mitochondrial F_1F_O-ATPase exploits the dithiol redox state to modulate the permeability transition pore.

Algieri C, Trombetti F, Pagliarani A, Ventrella V, Nesci S. Archives of Biochemistry and Biophysics. 2021; 712: 109027.

The final published version is available online at: **https://doi.org/10.1016/j.abb.2021.109027**

Rights / License:

The terms and conditions for the reuse of this version of the manuscript are specified in the publishing policy. For all terms of use and more information see the publisher's website.

This item was downloaded from IRIS Università di Bologna (https://cris.unibo.it/)

When citing, please refer to the published version.

Revised Manuscript Without Changes Marked

Click here to view linked References

The mitochondrial F_1F_O-ATPase exploits the dithiol redox state to modulate the permeability transition pore

Cristina Algieri, Fabiana Trombetti, Alessandra Pagliarani, Vittoria Ventrella, Salvatore Nesci*

Department of Veterinary Medical Sciences, University of Bologna, via Tolara di Sopra, 50 - 40064, Ozzano Emilia, Bologna, Italy

*Corresponding Author: Department of Veterinary Medical Sciences (DIMEVET), University of Bologna, via Tolara di Sopra, 50, 40064, Ozzano Emilia, Bologna, Italy; Tel. +39 051 2097004; Email: salvatore.nesci@unibo.it

ABSTRACT

The dithiol reagents phenylarsine oxide (PAO) and dibromobimane (DBrB) have opposite effects on the F_1F_O-ATPase activity. PAO 20% increases ATP hydrolysis at 50 µM when the enzyme activity is activated by the natural cofactor Mg^{2+} and at 150 µM when it is activated by Ca^{2+}. The PAO-driven F_1F_O-ATPase activation is reverted to the basal activity by 50 µM dithiothreitol (DTE). Conversely, 300 µM DBrB decreases the F_1F_O-ATPase activity by 25% when activated by Mg^{2+} and by 50% when activated by Ca^{2+}. In both cases, the F_1F_O-ATPase inhibition by DBrB is insensitive to DTE. The mitochondrial permeability transition pore (mPTP) formation, related to the Ca^{2+}-dependent F_1F_O-ATPase activity, is stimulated by PAO and desensitized by DBrB. Since PAO and DBrB apparently form adducts with different cysteine couples, the results highlight the crucial role of cross-linking of vicinal dithiols on the F_1F_O-ATPase, with (ir)reversible redox states, in the mPTP modulation.

Keywords: Mitochondria; F_1F_O-ATPase; mPTP; Thiols; Post-translational modification.

Introduction

The F_1F_O-ATPase by triggering the mitochondrial permeability transition pore (mPTP) provides the molecular entity of this biological phenomenon [1,2]. The mPTP formation, which triggers lethal events in the cell, is involved in physiological and pathological functions and known to be affected by oxidative stress that oxidizes and/or cross-links the protein thiols. Consequently, the cysteine redox state can favor/hamper the "open" mPTP conformation, in turn promoted by Ca^{2+} accumulation in the mitochondrial matrix. The mechanism(s) by which thiol oxidation promotes the mPTP formation was extensively investigated and may have biological implications in unravelling the mechanism of cell damage under oxidative stress [3]. Moreover, the recent observation of the different cryo-EM structure of the F_1F_O-ATPase in the presence of Mg^{2+} or Ca^{2+} as cation cofactor in the enzyme catalytic sites, highlighted the release of the lipid-plug from the *c*-ring in the "bent-pull" model [2,4]. In addition, Ca^{2+}-interactions with the F_1F_O-ATPase were proven to modulate the mPTP activity [5]. The mPTP opens under an abrupt increase in Ca^{2+} concentration in mitochondria. Under such conditions, the F_1F_O-ATPase replaces the natural cofactor Mg^{2+} with Ca^{2+}, which is probably only bound to the catalytic sites [6]. Ca^{2+} insertion promotes a conformational change within the enzyme structure, which is transmitted from the F_1 domain to membrane-embedded subunits of the F_O domain, thus triggering the pore formation in the mitochondrial membrane [7,8]. Accordingly, Ca^{2+} has higher atomic radius than Mg^{2+} and can establish different interactions and coordination numbers within the catalytic sites of the enzyme. The Ca^{2+} steric hindrance can modify the F_1 conformation and transmit a mechanical signal through the peripheral stalk to the membrane subunits of the F_O domain. Indeed, the Ca^{2+}-activated F_1F_O-ATPase assumes a disassembled conformation where F_1 is detached from F_O driven by a twisted form of the peripheral stalk (Fig. 1a).

Dithiol reagents with different features are a precious tool to evaluate how (ir)reversible post-translational modifications of di-thiols on F_1F_O-ATPase [9] affect the formation and regulation of the mPTP. Phenylarsine oxide (PAO) and dibromobimane (DBrB) are sulfhydryl (-SH) group modifiers that cause intramolecular cross-linking between two vicinal cysteine thiols [10]. PAO is an hydrophobic reagent and can directly react with functional -SH groups of the mPTP that are inaccessible to hydrophilic reagents in the absence of Ca^{2+} [11]. Moreover, PAO selectively binds to vicinal thiols to form a stable dithioarsine ring and dramatically decreases the mPTP induction time in isolated mitochondria [12]. This abbreviation even occurs in the presence of excess EGTA (Ca^{2+} chelator) in non-respiring mitochondria [11]. The threshold potential for mPTP opening is modulated by the mitochondrial redox state through both pyridine nucleotide pool ($NADH/NAD^+$ and $NADPH/NADP^+$) and -SH groups (presumably by glutathione action) [13]. DBrB, which cross-links neighbouring cysteine residues, decreased the oligomycin-sensitive (OS)-ATPase to -35% of the control activity in beef heart mitochondria [14] by forming a protein-DBrB adduct. Conversely, DBrB cannot establish a thiol bridge when the protein already forms an intra protein disulfide [10]. Disulfides are featured by the thiol-thiol bond length, namely the distance between the two thiols (-S-S- distance). Disulfide bonds are usually about 2.05 Å in length, and 3.0 Å is taken as the cut-off for disulfides in the PDB database [15]. The capacity to join dithiols depends on the molecular structure of the cross-linked compound (*X*) which establishes sulfide bridges (-S–*X*–S-) of different lengths [16]. Indeed, DBrB can cover a broader distance between vicinal thiols than PAO (Fig. 1b).

The assessment of the dithiol reagents action mechanism on the F_1F_O-ATPase may be extremely useful to adequately exploit properties of the redox state of thiol groups for medical purposes.

Material and methods

Chemicals

Oligomycin (a mixture of oligomycins A, B and C), and Fura-FF were purchased from Vinci-Biochem (Vinci, Italy). Na_2ATP, Phenylarsine oxide (PAO), Dibromobimane (DBrB), and 1,4-Dithioerythritol (DTE) were obtained from Sigma–Aldrich (Milan, Italy). Quartz double distilled water was used for all reagent solutions.

Preparation of the mitochondrial fractions

Swine hearts (*Sus scrofa domesticus*) were collected at a local abattoir and transported to the lab within 2 h in ice buckets at 0–4 °C. After removal of fat and blood clots as much as possible, approximately 30–40 g of heart tissue was rinsed in ice-cold washing Tris-HCl buffer (medium A) consisting of 0.25 M sucrose, 10 mM Tris(hydroxymethyl)-aminomethane (Tris), pH 7.4 and finely chopped into fine pieces with scissors. Each preparation was made from one heart. Once rinsed, tissues were gently dried on blotting paper and weighted. Then tissues were homogenized in medium B consisting of 0.25 M sucrose, 10 mM Tris, 1 mM EDTA (free acid), 0.5 mg/ml BSA fatty acid-free, pH 7.4 with HCl at a ratio of 10 ml medium B per 1 g of fresh tissue. After a preliminary gentle break up by Ultraturrax T25, the tissue was carefully homogenized by a motor-driven Teflon pestle homogenizer (Braun Melsungen Type 853202) at 650 rpm with 3 up-and-down strokes. The mitochondrial fraction was then obtained by stepwise centrifugation (Sorvall RC2-B, rotor SS34). Briefly, the homogenate was centrifuged at 1000×*g* for 5 min, thus yielding a supernatant and a pellet. The pellet was re-homogenized under the same conditions of the first homogenization and re-centrifuged at 1000×*g* for 5 min. The gathered supernatants from these two centrifugations, filtered through four cotton gauze layers, were centrifuged at 10,500×*g* for 10 min to yield the raw mitochondrial pellet. The raw pellet was resuspended in medium A and further centrifuged at 10,500×*g* for 10 min to obtain the final mitochondrial pellet. The latter was resuspended by gentle stirring using a Teflon Potter Elvejehm homogenizer in a small volume of medium A, thus obtaining a protein concentration of 30 mg/ml [17]. All steps were carried out at 0–4 °C. The protein concentration was determined according to the colorimetric method of Bradford by Bio-Rad Protein Assay kit II with BSA as standard. The mitochondrial preparations were then stored in liquid nitrogen until the evaluation of F_1F_O-ATPase activities.

Mitochondrial F-ATPase activity assays

Thawed mitochondrial preparations were immediately used for F-ATPase activity assays. The capability of ATP hydrolysis was assayed in a reaction medium (1 ml). The optimal conditions to obtain the maximal activity of the F_1F_O-ATPase, which depend on substrates concentration and pH values, are at 0.15 mg mitochondrial protein and 75 mM ethanolamine–HCl buffer pH 9.0, 6.0 mM Na_2ATP and 2.0 mM $MgCl_2$ for the Mg^{2+}-activated F_1F_O-ATPase assay, and 75 mM ethanolamine–HCl buffer pH 8.8, 3.0 mM Na_2ATP and 2.0 mM $CaCl_2$ for the Ca^{2+}-activated F_1F_O-ATPase assay. These assay conditions were previously proven to elicit the maximal enzyme activities either stimulated by Mg^{2+} or by Ca^{2+} in swine heart mitochondria [5]. After 5 min preincubation at 37 °C, the reaction, carried out at the same temperature, was started by the addition of the substrate Na_2ATP and stopped after 5 min by the addition of 1 ml of ice-cold 15% (w/w) trichloroacetic acid (TCA) aqueous solution. Once the reaction was stopped, vials were centrifuged for 15 min at 3500 rpm (Eppendorf Centrifuge 5202). In the supernatant, the concentration of inorganic phosphate (Pi) hydrolyzed by known amounts of mitochondrial protein, which is an indirect measure of F-ATPase activity, was spectrophotometrically evaluated [18]. According to the method employed, to detect the Pi release by the enzymatic reaction, the Pi released independently of the F_1F_O-ATPase activity should be quantified. To this aim, 1 µl from a stock solution of 3 mg/ml oligomycin in dimethylsulfoxide was directly added to the reaction mixture before starting the reaction. The total mitochondrial ATPase activity was calculated by detecting the Pi in control tubes run in parallel and containing 1 µl dimethylsulfoxide per ml reaction system. In each experimental set, control tubes were alternated to the condition to be tested. The employed dose of

oligomycin, a specific inhibitor of F-ATPases which selectively blocks the F_O subunit ensured maximal enzyme activity inhibition and was currently used in F-ATPase assays [19].

In all experiments, the F_1F_O-ATPase activity was routinely measured by subtracting, from the Pi hydrolyzed by the total ATPase activity, the Pi hydrolyzed in the presence of oligomycin [20]. In all experiments the F-ATPase activity, either activated by Ca^{2+} as a cofactor or by Mg^{2+}, was expressed as μmol Pi·mg protein^{-1}·min^{-1}.

Evaluation of PTP

Immediately after the preparation of swine heart mitochondrial fractions, fresh mitochondrial suspensions (1 mg/ml) were energized in the assay buffer (130 mM KCl, 1 mM KH_2PO_4, 20 mM HEPES, pH 7.2 with TRIS), incubated at 25 °C with 1 μg/ml rotenone and 5 mM succinate as respiratory substrate. To evaluate PAO or DBrB effect, selected di-thiol group cross-linking reagents concentrations, obtained by sampling small aliquots from standard PAO or DBrB aqueous solutions, as described in the Section "Mitochondrial F-ATPase activity assays", were added to the mitochondrial suspensions before mPTP evaluation. mPTP opening was induced by the addition of low concentrations of Ca^{2+} (10 μM) as $CaCl_2$ aqueous solution at fixed time intervals (1 min). The Ca^{2+} retention capacity (CRC), whose lowering indicates mPTP opening, was spectrofluorophotometrically evaluated in the presence of 0.8 μM Fura-FF. The probe has different spectral properties in the absence and in the presence of Ca^{2+}, namely, it displays excitation/emission spectra of 365/514 nm in the absence of Ca^{2+} (Fura-FF low Ca^{2+}) and shifts to 339/507 nm in the presence of high Ca^{2+} concentrations (Fura-FF high Ca^{2+}). mPTP opening was evaluated by the increase in the fluorescence intensity ratio (Fura-FF high Ca^{2+})/(Fura-FF low Ca^{2+}), which indicates a decrease in CRC [5]. All measurements were processed by LabSolutions RF software.

Calculations and statistics

The data represent the mean±SD (shown as vertical bars in the figures) of the number of experiments reported in the figure captions. In each experimental set, the analyses were carried out on different pools of animals. Statistical analyses were performed by SIGMASTAT software. The analysis of variance followed by Students–Newman–Keuls' test when *F* values indicated significance ($P \leq 0.05$) was applied. Percentage data were arcsin-transformed before statistical analyses to ensure normality.

Results and Discussion

In swine heart mitochondria the bifunctional thiol reagents PAO and DBrB show opposite effects on the F_1F_O-ATPase activity. PAO 20% increases the activity of the F_1F_O-ATPase either activated by Mg^{2+} or by Ca^{2+} at 50 μM and 150 μM, respectively (Fig. 2A). Conversely, DBrB shows a maximal 25% inhibition of the Mg^{2+}-activated F_1F_O-ATPase at 150 μM DBrB, and a maximal 50% inhibition of the Ca^{2+}-activated F_1F_O-ATPase at 300 μM DBrB (Fig. 2B). The opposite effect of the two dithiol reagents may be due to their interaction with different cysteine couples of the enzyme. Therefore, the post-traslational cysteine modifications could alter the F_1F_O-ATPase structure independently of which cation activates the enzyme. Disulfide forms on the F_1F_O-ATPase by binding between Cys251 of two α subunits or Cys251 and Cys78 of α and γ subunit, respectively during holoenzyme assembly [21]. The disulfur cross-link between cysteines is associated with F_1F_O-ATPase dysfunction in heart failure patients [21]. Conversely, reversible dithiol bridges, established by mercury, increase the F_1F_O-ATPase activity when the MgATP substrate is bound in the catalytic sites [22].

To verify if the cysteine oxidation by PAO and DBrB was related to their opposite effects on the F_1F_O-ATPase the reducing thiol reagent DTE was tested. The Mg^{2+}- or Ca^{2+}-activated F_1F_O-ATPase the activities were evaluated in the presence of 150 μM PAO (Fig. 3A,B) or 300 μM DBrB (Fig. 3C,D) with and without DTE to check if the modified cysteine thiols (-S–*X*–S-) of the protein adduct were reduction-sensitive. In the presence of 50 μM DTE the Mg^{2+}- and Ca^{2+}-activated F_1F_O-ATPase showed the same enzyme activity as the control in a PAO- and DTE-free reaction medium (Fig. 3A,C) or in a DBrB- and DTE-free reaction medium (Fig. 3B,D). The 50 μM DTE addition significantly lessened the 20% Mg^{2+}- or Ca^{2+}-activated F_1F_O-ATPase stimulation in the presence of PAO (Fig. 3A,B). Conversely, in the presence of DBrB, the Mg^{2+}- or Ca^{2+}-activated F_1F_O-ATPase inhibition by 25% and 50%, respectively were maintained irrespective of DTE (Fig. 3C,D). The respective reversible and irreversible redox behaviour of PAO- or DBrB-sensitive cysteine couples confirms that this regulation is irrespective of the cofactor bound to the catalytic sites. Oxidative stress causes a variety of post-translational modifications of thiol groups. The thiol-bearing cysteines are unique molecular switches which play structural and regulatory roles in biology [23] and in mitochondria that are an highly compartmentalized thiol-redox organelles [24]. The PAO and DBrB effects highlight how different dithiol modifiers act on the F_1F_O-ATPase catalytic activity and on the known redox state of vicinal cysteinyl residues in tuning the mPTP opening and the F_1F_O-ATPase, thus reinforcing their mutual link [25]. Indeed, the calcium retention capacity (CRC), by measuring the capability of intact mitochondria to accumulate Ca^{2+} and to release it when the mPTP opens, showed opposite profiles in the presence of PAO and DBrB (Fig. 4), consistently with the F_1F_O-ATPase modulation by these reagents. In other words, in CRC assays the addition of Ca^{2+} pulses make Ca^{2+} accumulate in the mitochondrial matrix so as mitochondria take up Ca^{2+}. The decreased Ca^{2+} accumulation in mitochondria shown by CRC drop reflects the mPTP opening. Therefore, the CRC decrease in PAO- treated mitochondria, revealed by an increase in fluorescence intensity detected as Fura-FF ratio [(Fura-FF high Ca^{2+})/(Fura-FF low Ca^{2+})], points out that PAO sensitizes the mPTP formation to Ca^{2+} and, consistently, stimulates the F_1F_O-ATPase activities. The PAO-driven increased mPTP sensitivity was counteracted by DTE, thus confirming the involvement of cross-linked critical dithiols in mPTP opening. The DBrB concentration tested (300 μM), selected on the basis of the 50% inhibition of the Ca^{2+}-activated F_1F_O-ATPase whose activity is related to the mPTP opening [25–28], did not elicit any sudden increase in fluorescence intensity due to Ca^{2+} release. Moreover, the mPTP inhibition by DBrB was insensitive to DTE (Fig. 4). The DBrB inhibition of mPTP formation was corroborated by the inhibition of the two F_1F_O-ATPase activities, especially of the Ca^{2+} activated F_1F_O-ATPase.

We can infer that two different cysteine couples specifically cross-linked with PAO and DBrB produce opposite effects on the F_1F_O-ATPase and on the mPTP. Moreover, apparently DTE only reduces the dithiols that react with PAO, whereas it can remove the irreversible inhibition caused by DBrB. It is tempting to speculate that the F_1F_O-ATPase has two distinct molecular strategies to regulate the mPTP opening: *i*) the reversible oxidation of vicinal dithiols (presumably not farther than 3.8 Å (Fig. 1B)); *ii*) the irreversible oxidation of dithiols far up to 6.6 Å from each other (Fig. 1B). Since, the mPTP participates in both development and cell death [29], the dithiols by post-translational modification may act on the regulation of the transition from physiological to pathological mPTP opening in mitochondria. In this perspective, future studies could point out cysteine pairs on the F_1F_O-ATPase which may serve as drug targets to control pathological conditions due to mPTP dysregulation and, physiologically, are molecular keys to open the mPTP.

Author Contributions

C.A. investigation and formal analysis; F.T. and V.V. validation; F.T. and A.P. resources and writing—review & editing; S.N. conceptualization, supervision and writing—original draft.

ACKNOWLEDGMENTS

This study was supported by a RFO grant from the University of Bologna, Italy

Danilo Matteuzzi and Roberto Giusti (Department of Veterinary Medical Sciences, University of Bologna) are gratefully acknowledged for kindly conferring swine hearts from a local abattoir to Biochemistry laboratories.

REFERENCES

[1] S. Nesci, A. Pagliarani, Emerging Roles for the Mitochondrial ATP Synthase Supercomplexes, Trends Biochem. Sci. 44 (2019) 821–823. https://doi.org/10.1016/j.tibs.2019.07.002.

[2] G. Pinke, L. Zhou, L.A. Sazanov, Cryo-EM structure of the entire mammalian F-type ATP synthase, Nat Struct Mol Biol. 27 (2020) 1077–1085. https://doi.org/10.1038/s41594-020-0503-8.

[3] V. Petronilli, P. Costantini, L. Scorrano, R. Colonna, S. Passamonti, P. Bernardi, The voltage sensor of the mitochondrial permeability transition pore is tuned by the oxidation-reduction state of vicinal thiols. Increase of the gating potential by oxidants and its reversal by reducing agents, J. Biol. Chem. 269 (1994) 16638–16642.

[4] N. Mnatsakanyan, E.A. Jonas, ATP synthase c-subunit ring as the channel of mitochondrial permeability transition: Regulator of metabolism in development and degeneration, J. Mol. Cell. Cardiol. 144 (2020) 109–118. https://doi.org/10.1016/j.yjmcc.2020.05.013.

[5] C. Algieri, F. Trombetti, A. Pagliarani, M. Fabbri, S. Nesci, The inhibition of gadolinium ion (Gd3+) on the mitochondrial F1FO-ATPase is linked to the modulation of the mitochondrial permeability transition pore, International Journal of Biological Macromolecules. 184 (2021) 250–258. https://doi.org/10.1016/j.ijbiomac.2021.06.065.

[6] M.J. Hubbard, N.J. McHugh, Mitochondrial ATP synthase F1-beta-subunit is a calcium-binding protein, FEBS Lett. 391 (1996) 323–329.

[7] S. Nesci, F. Trombetti, V. Ventrella, A. Pagliarani, From the Ca2+-activated F1FO-ATPase to the mitochondrial permeability transition pore: an overview, Biochimie. 152 (2018) 85–93. https://doi.org/10.1016/j.biochi.2018.06.022.

[8] V. Giorgio, V. Burchell, M. Schiavone, C. Bassot, G. Minervini, V. Petronilli, F. Argenton, M. Forte, S. Tosatto, G. Lippe, P. Bernardi, Ca(2+) binding to F-ATP synthase β subunit triggers the mitochondrial permeability transition, EMBO Rep. 18 (2017) 1065–1076. https://doi.org/10.15252/embr.201643354.

[9] S. Nesci, F. Trombetti, V. Ventrella, A. Pagliarani, Post-translational modifications of the mitochondrial F1FO-ATPase, Biochim. Biophys. Acta. 1861 (2017) 2902–2912. https://doi.org/10.1016/j.bbagen.2017.08.007.

[10] O. Rudyk, P. Eaton, Biochemical methods for monitoring protein thiol redox states in biological systems, Redox Biol. 2 (2014) 803–813. https://doi.org/10.1016/j.redox.2014.06.005.

[11] E. Lenartowicz, P. Bernardi, G.F. Azzone, Phenylarsine oxide induces the cyclosporin A-sensitive membrane permeability transition in rat liver mitochondria, Journal of Bioenergetics and Biomembranes. 23 (1991) 679–688. https://doi.org/10.1007/BF00785817.

[12] P. Bernardi, S. Vassanelli, P. Veronese, R. Colonna, I. Szabó, M. Zoratti, Modulation of the mitochondrial permeability transition pore. Effect of protons and divalent cations, J Biol Chem. 267 (1992) 2934–2939.

[13] P. Costantini, B.V. Chernyak, V. Petronilli, P. Bernardi, Modulation of the mitochondrial permeability transition pore by pyridine nucleotides and dithiol oxidation at two separate sites, J. Biol. Chem. 271 (1996) 6746–6751.

[14] G. Zimmer, L. Mainka, B.M. Heil, Bromobimane crosslinking studies in oligomycin-sensitive ATPase from beef heart mitochondria. Mr 31 000 protein crosslinked, FEBS Lett. 150 (1982) 207–210. https://doi.org/10.1016/0014-5793(82)81335-5.
[15] M.-A. Sun, Y. Wang, Q. Zhang, Y. Xia, W. Ge, D. Guo, Prediction of reversible disulfide based on features from local structural signatures, BMC Genomics. 18 (2017) 279. https://doi.org/10.1186/s12864-017-3668-8.
[16] A. Shvetsov, J.D. Stamm, M. Phillips, D. Warshaviak, C. Altenbach, P.A. Rubenstein, K. Hideg, W.L. Hubbell, E. Reisler, Conformational Dynamics of Loop 262−274 in G- and F-actin, Biochemistry. 45 (2006) 6541–6549. https://doi.org/10.1021/bi052558v.
[17] S. Nesci, V. Ventrella, F. Trombetti, M. Pirini, A. Pagliarani, Preferential nitrite inhibition of the mitochondrial F1FO-ATPase activities when activated by Ca(2+) in replacement of the natural cofactor Mg(2+), Biochim. Biophys. Acta. 1860 (2016) 345–353. https://doi.org/10.1016/j.bbagen.2015.11.004.
[18] V. Ventrella, S. Nesci, F. Trombetti, P. Bandiera, M. Pirini, A.R. Borgatti, A. Pagliarani, Tributyltin inhibits the oligomycin-sensitive Mg-ATPase activity in Mytilus galloprovincialis digestive gland mitochondria, Comp. Biochem. Physiol. C Toxicol. Pharmacol. 153 (2011) 75–81. https://doi.org/10.1016/j.cbpc.2010.08.007.
[19] S. Nesci, V. Ventrella, F. Trombetti, M. Pirini, A. Pagliarani, The mitochondrial F1FO-ATPase desensitization to oligomycin by tributyltin is due to thiol oxidation, Biochimie. 97 (2014) 128–137. https://doi.org/10.1016/j.biochi.2013.10.002.
[20] S. Nesci, V. Ventrella, F. Trombetti, M. Pirini, A. Pagliarani, Tri-n-butyltin binding to a low-affinity site decreases the F1FO-ATPase sensitivity to oligomycin in mussel mitochondria, Applied Organometallic Chemistry. 26 (2012) 593–599. https://doi.org/10.1002/aoc.2904.
[21] S.-B. Wang, D.B. Foster, J. Rucker, B. O'Rourke, D.A. Kass, J.E. Van Eyk, Redox regulation of mitochondrial ATP synthase: implications for cardiac resynchronization therapy, Circ. Res. 109 (2011) 750–757. https://doi.org/10.1161/CIRCRESAHA.111.246124.
[22] S. Nesci, F. Trombetti, M. Pirini, V. Ventrella, A. Pagliarani, Mercury and protein thiols: Stimulation of mitochondrial F1FO-ATPase and inhibition of respiration, Chem. Biol. Interact. 260 (2016) 42–49. https://doi.org/10.1016/j.cbi.2016.10.018.
[23] A. Fra, E.D. Yoboue, R. Sitia, Cysteines as Redox Molecular Switches and Targets of Disease, Front Mol Neurosci. 10 (2017) 167. https://doi.org/10.3389/fnmol.2017.00167.
[24] S. Dröse, U. Brandt, I. Wittig, Mitochondrial respiratory chain complexes as sources and targets of thiol-based redox-regulation, Biochim Biophys Acta. 1844 (2014) 1344–1354. https://doi.org/10.1016/j.bbapap.2014.02.006.
[25] C. Algieri, F. Trombetti, A. Pagliarani, V. Ventrella, C. Bernardini, M. Fabbri, M. Forni, S. Nesci, Mitochondrial Ca2+ -activated F1 FO -ATPase hydrolyzes ATP and promotes the permeability transition pore, Ann. N. Y. Acad. Sci. 1457 (2019) 142–157. https://doi.org/10.1111/nyas.14218.
[26] C. Algieri, F. Trombetti, A. Pagliarani, V. Ventrella, S. Nesci, Phenylglyoxal inhibition of the mitochondrial F1FO-ATPase activated by Mg2+ or by Ca2+ provides clues on the mitochondrial permeability transition pore, Arch. Biochem. Biophys. 681 (2020) 108258. https://doi.org/10.1016/j.abb.2020.108258.
[27] S. Nesci, C. Algieri, F. Trombetti, V. Ventrella, M. Fabbri, A. Pagliarani, Sulfide affects the mitochondrial respiration, the Ca2+-activated F1FO-ATPase activity and the permeability transition pore but does not change the Mg2+-activated F1FO-ATPase activity in swine heart mitochondria, Pharmacol Res. 166 (2021) 105495. https://doi.org/10.1016/j.phrs.2021.105495.
[28] V. Algieri, C. Algieri, L. Maiuolo, A. De Nino, A. Pagliarani, M.A. Tallarida, F. Trombetti, S. Nesci, 1,5-Disubstituted-1,2,3-triazoles as inhibitors of the mitochondrial Ca2+ -activated F1 FO -ATP(hydrol)ase and the permeability transition pore, Ann N Y Acad Sci. 1485 (2021) 43–55. https://doi.org/10.1111/nyas.14474.
[29] M.J. Pérez, R.A. Quintanilla, Development or disease: duality of the mitochondrial permeability transition pore, Dev. Biol. 426 (2017) 1–7. https://doi.org/10.1016/j.ydbio.2017.04.018.
[30] S. Nesci, A. Pagliarani, Incoming news on the F-type ATPase structure and functions in mammalian mitochondria, BBA Advances. 1 (2021) 100001. https://doi.org/10.1016/j.bbadva.2020.100001.

FIGURE

Figure 1. Molecular mechanism. A) Model of F_1F_O-ATPase in the mPTP formation. The F_1F_O-ATPase activity sustained by the Ca^{2+} as cofactor hydrolyzes ATP by causing disassembly/distortion of the entire enzyme complex. The structural modification of the Ca^{2+}-activated F_1F_O-ATPase triggers the formation and opening of the mPTP [2,30]. B) Reactions involved in the dithiol bridge formation by phenylarsine oxide (PAO) and dibromobimane (DBrB). The distances between two thiol groups linked by the reagent *X* (-S–*X*–S-) were calculated by Chem3D.

Figure 2. Dose-response curve of di-thiol cross-linking reagents on the F_1F_O-ATPase activity. Effect of increasing PAO (A) or DBrB (B) concentrations on the F_1F_O-ATPase activated by Mg^{2+} (Mg^{2+}-activated F_1F_O-ATPase) (●) and by Ca^{2+} (Ca^{2+}-activated F_1F_O-ATPase) (○) activities. Data represent the mean ± SD from three independent experiments carried out on three different mitochondrial preparations.

Figure 3. Mg^{2+} and Ca^{2+}-activated F_1F_O-ATPase activities in PAO or DBrB-treated mitochondria in the presence of thiol reducing (50 µM DTE) agent. The effect of 150 µM PAO (A and B) or 150 µM DBrB (C and D) was evaluated in the absence (green bars,) and in the presence (red bars,) of DTE. Data represent the mean ± SD from three independent experiments carried out on three different mitochondrial preparations. Different letters indicate significantly different values within each treatment ($P \leq 0.05$).

Figure 4. Evaluation of PTP opening in intact mitochondrial preparations. CRC, detected as Fura-FF ratio, was monitored in response to subsequent 10 µM $CaCl_2$ pulses (shown by the arrows), as detailed in the Section Methods, in the absence (Control-black line, —) and in the presence of 150 µM PAO (light blue line, —), 150 µM DBrB (red line, —), 150 µM PAO + 50 µM DTE (gold line, —), and 150 µM DBrB + 50 µM DTE (green line, —). The PAO and DBrB concentrations were selected based on the maximal activation or inhibition of the Ca^{2+}-activated F_1F_O-ATPase by PAO or DBrB, respectively. Three independent experiments were carried out on three different mitochondrial preparations.

Figure 1

Click here to access/download;Figure;Figure 1.tif

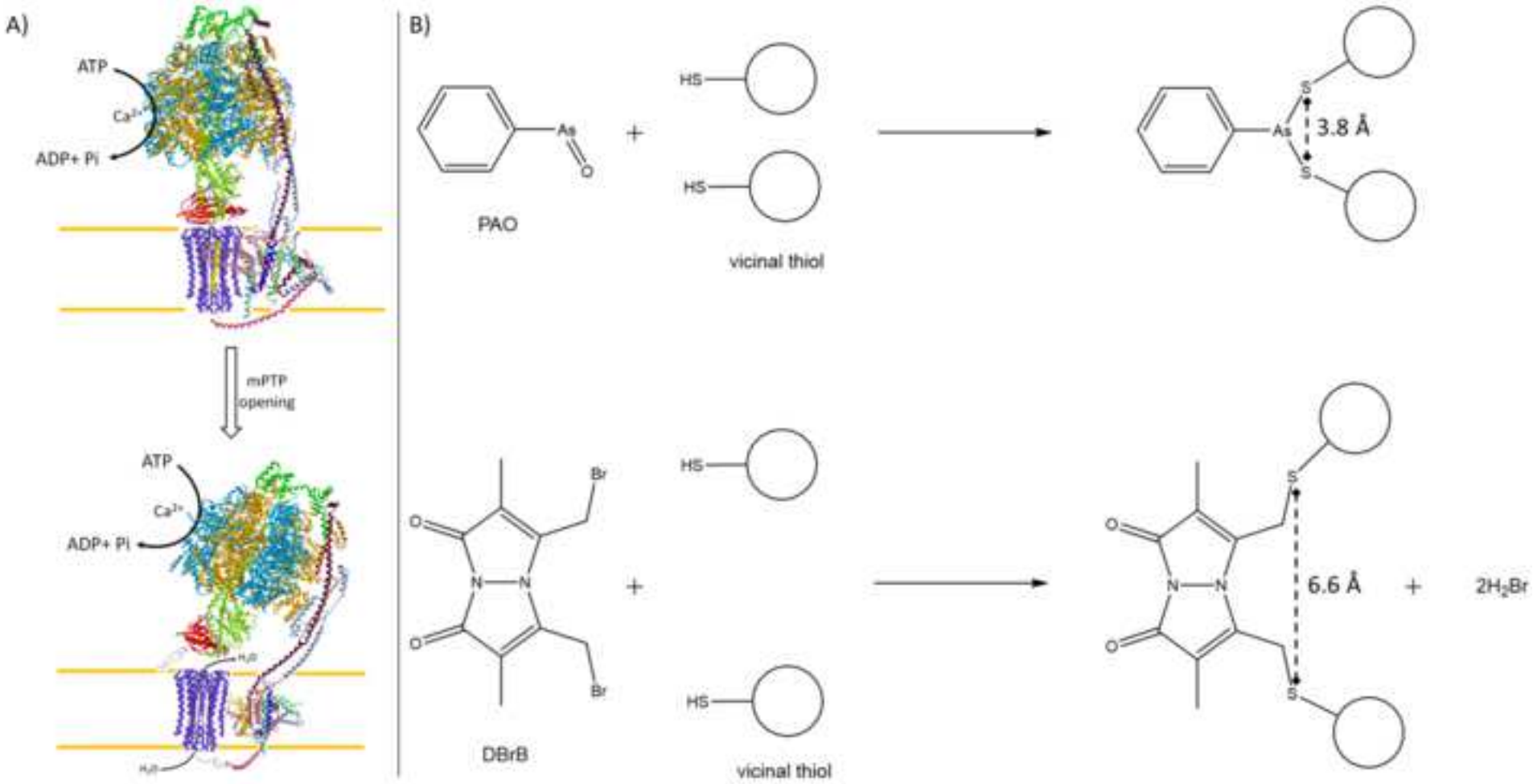

Figure 2

Click here to access/download;Figure;Figure 2.tif

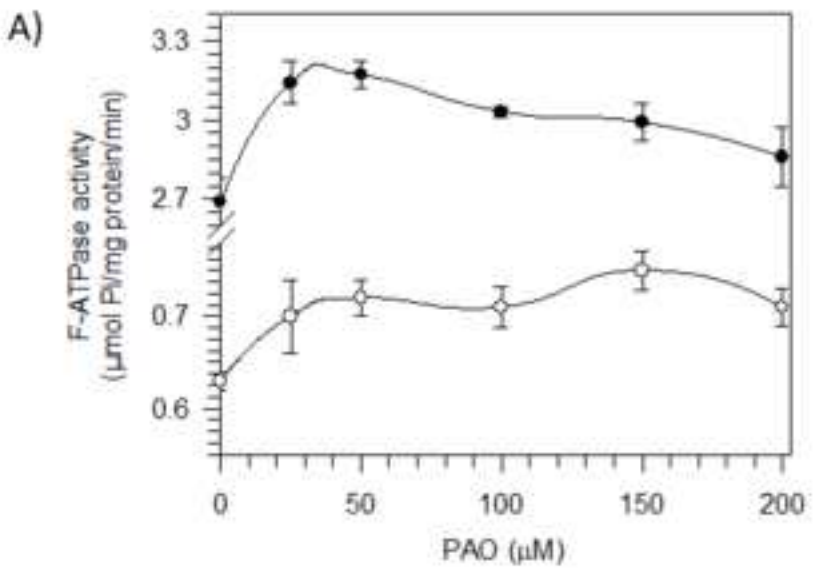

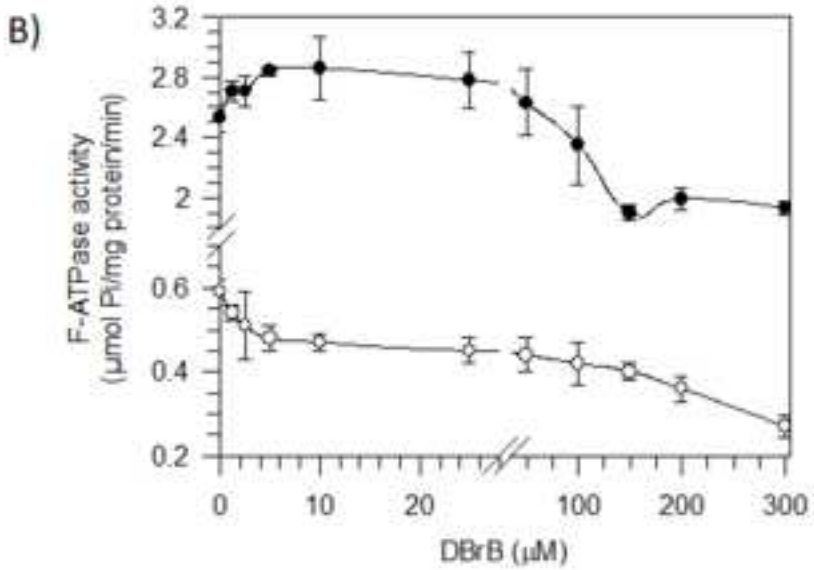

Figure 3

Click here to access/download;Figure;Figure 3.tif

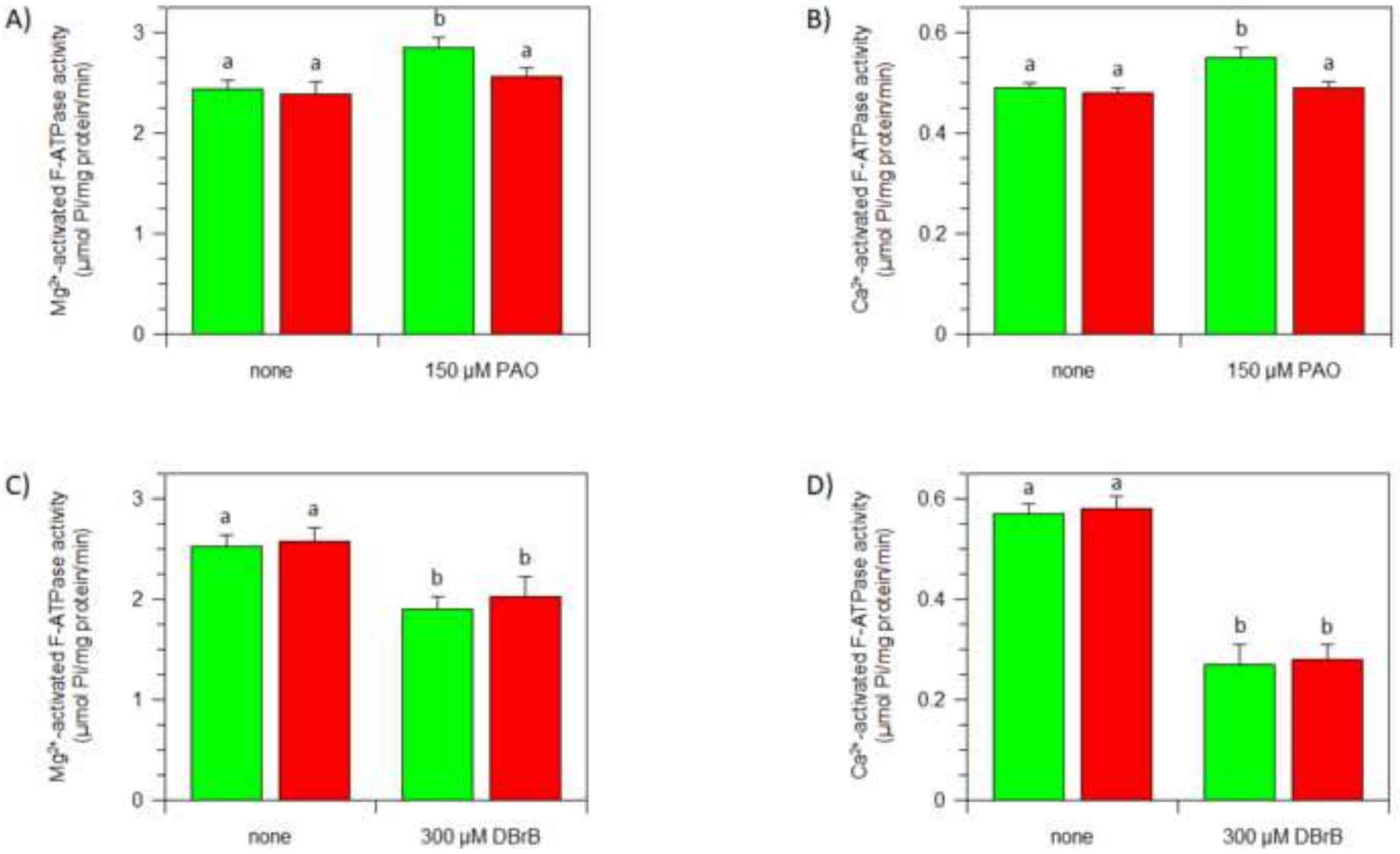

Figure 4
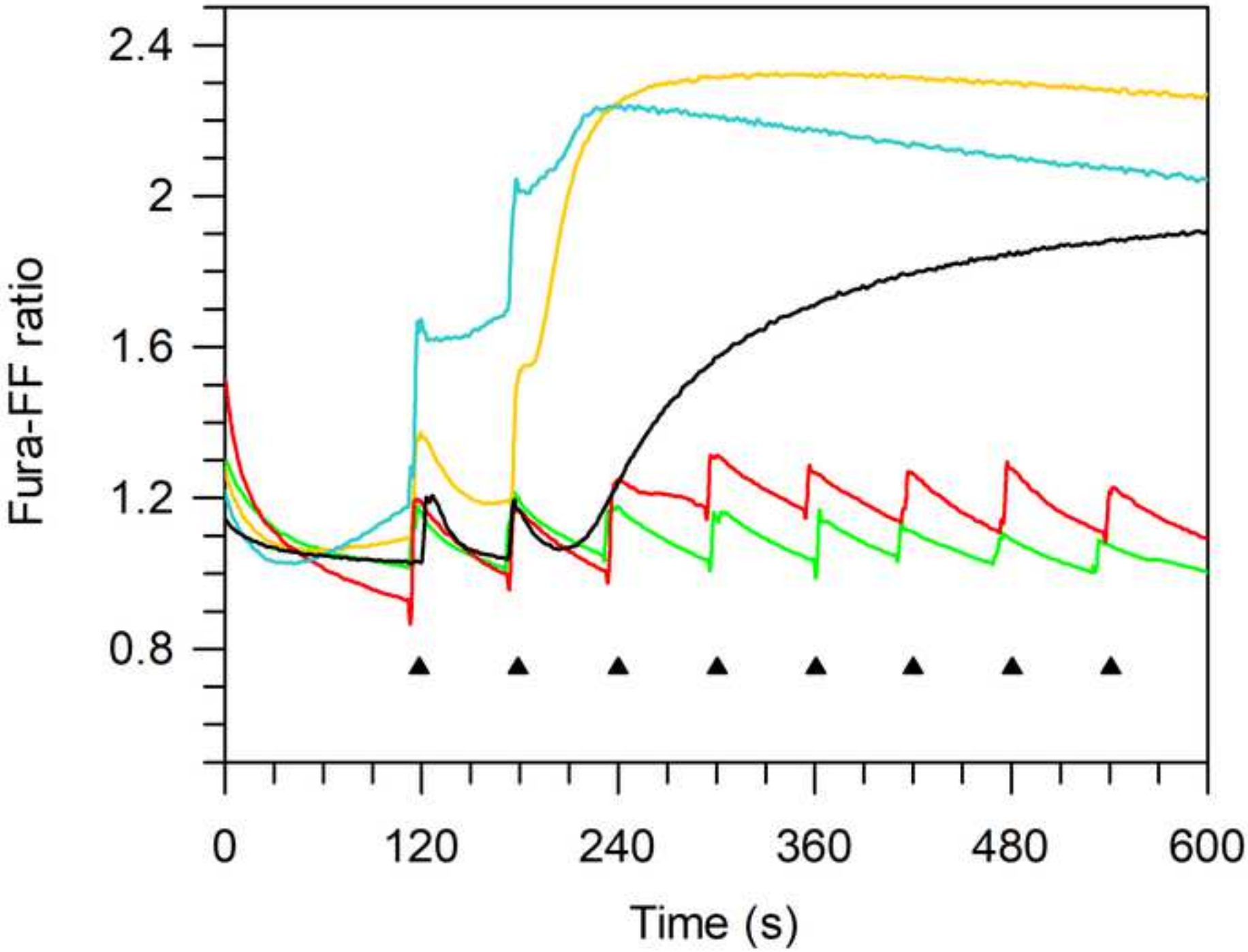
Click here to access/download;Figure;Figure 4.tif